

Raman Regime Energy Dependence of Alignment and Orientation of KrII States Populated by Resonant Auger Effect

B. M. Lagutin, I. D. Petrov, and V. L. Sukhorukov*

Rostov State University of Transport Communications, 344038 Rostov-on-Don, Russia

S. Kammer, S. Mickat, R. Schill, and K.-H. Schartner

I. Physikalisches Institut, Justus-Liebig-Universität, D-35392 Giessen, Germany

A. Ehresmann, Yu. A. Shutov, and H. Schmoranzer†

Fachbereich Physik, Universität Kaiserslautern, D-67653 Kaiserslautern, Germany

(Received 30 July 2002; published 18 February 2003)

The energy dependencies of alignment parameters A_{20} for KrII $4p^45p$ states after the Auger decay of the KrI $3d^9np$ resonances were investigated theoretically and experimentally for the first time in the Raman regime with the bandwidth of the exciting radiation ($\Delta E_{\text{FWHM}} = 20$ meV) smaller than the natural width of the resonances ($\Gamma \approx 80$ meV). The observed energy dependence is due to the interference between the different resonance channels and the direct photoionization channel. A strong energy dependence for both the orientation parameter O_{10} and the photoelectron angular distribution parameter β_{el} is also predicted.

DOI: 10.1103/PhysRevLett.90.073001

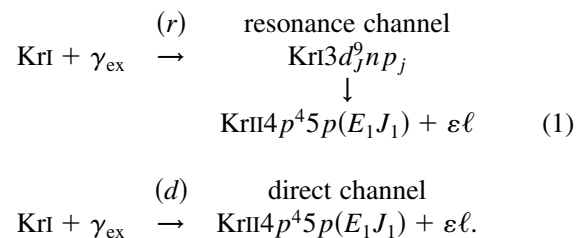
PACS numbers: 31.25.Jf, 32.80.Dz, 32.80.Fb

The resonant Auger effect (RA) leading to the population of KrII $4p^4np$ states (XeII $5p^4np$ states) after autoionization of the KrI $3d^9np$ resonances (XeI $4d^9np$ resonances) was reported for the first time about 25 years ago [1]. Thereafter, the RA has been utilized to study the dynamics of many-electron processes in different atoms and molecules in hundreds of articles (see the review [2]). The wide interest in the RA is largely based on the fact that the resonance population of the final ionic states is assumed to be considerably stronger than the direct non-resonant population. Therefore, it was expected that the dynamics of RA can be understood within a relatively simple two-step (or stepwise) model [3–5]. In this model, the direct population of the ionic states is neglected because it is forbidden in a single-electron dipole approximation and has a very small probability in comparison with the resonance channel. This is in marked contrast to the cases where direct and resonance channels are comparable and yield the complex dispersion of the spectroscopically observed quantities (see, e.g., [6–8]). The stepwise model has been applied to explain the measured Auger electron angular distribution [3–5] and the alignment of the ionic states [9,10] after the decay of the md^9np resonances in rare gas atoms.

The stepwise model is up to now the only one which is used in *ab initio* calculations of the RA dynamics, whereas its inadequacy for treating the branching ratio of different partial photoionization channels has recently been pointed out [11–13]. Therefore, in this Letter we investigate the influence of the interference between photoionization via the KrI $3d^9np$ resonances and the direct photoionization into the KrII $4p^4np$ states on the RA dynamics. The results predicted

by the calculations are tested by A_{20} measurements for selected KrII $4p^4np$ states performed in the Raman regime [14].

The processes relevant for the present work are summarized by the following scheme:



After the interaction of the ground state KrI with a linearly (circularly) polarized photon γ_{ex} , the KrI $3d^9np$ -resonance state is fully aligned (oriented). Alignment and orientation are then shared between the KrII $4p^45p$ state and the photoelectron $\varepsilon\ell$ during the Auger process, providing the proper angular distribution of the photoelectron and the alignment and orientation of the residual ion. The latter can be determined by measuring the polarization of the fluorescence γ_{fl} emitted in the $5p \rightarrow 5s$ transition. Of course, the direct photoionization channel (*d*) also influences the β_{el} and the alignment (orientation) of the KrII $4p^45p$ states. However, in the previous calculations [3–5] this channel has been completely neglected. In this Letter the direct channel (*d*) is included in the calculations for the first time and it will be shown that for selected KrII $4p^45p$ states in spite of its weakness it changes notably the results of the calculated quantities β_{el} , A_{20} , and O_{10} and brings them in closer agreement to measured data.

The expressions for the electron angular distribution parameter β_{el} , alignment A_{20} , and orientation O_{10} in dependence on the kinematics coefficients and the transition amplitudes have been given elsewhere [3–5,9,15,16]. The transition amplitudes determining the dynamics of all processes (1) are given by:

$$D(E_1 J_1, \varepsilon \ell) = \langle E_1 J_1, \varepsilon \ell | \mathbf{d} | 0 \rangle + \sum_R \frac{\langle E_1 J_1, \varepsilon \ell | \mathbf{H}^{ee} | R \rangle \langle R | \mathbf{d} | 0 \rangle}{(\varepsilon + E_1 - E) + i\Gamma(R)/2}, \quad (2)$$

where \mathbf{H}^{ee} and \mathbf{d} are the Coulomb and the transition operators, respectively; $\Gamma(R)$ is the total width of the resonance equal to 83 meV [17,18]. The first term entering Eq. (2) describes the direct photoionization, and the sum over R in the second term includes all resonance channels. It is clear that the stepwise model includes the single resonance term only in transition amplitude (2).

Wave functions for the KrII $4p^4 5p(E_1 J_1)$ states as well as for the resonance states KrI $3d^9 n p_j$ were computed within the configuration-interaction Pauli-Fock approximation [19] and were used in the calculation of all the above quantities. For the states KrII $4p^4 5p$ the same wave functions as in [9] have been used. The calculation of the wave functions for the KrI $3d^9 n p_j$ states is a more difficult task than for the lowest KrI $3d^9 5p_{3/2}$ state

(R1) which is practically a pure $|5/2, 3/2, J_R = 1\rangle$ state of jj coupling. In the computation of the KrI $3d^9 n p_j$ wave functions, the interaction of KrI $3d^9 5p_j$ ($j = 1/2, 3/2$) and KrI $3d^9 6p_{3/2}$ configurations is important. Accounting for this interaction yields three multiconfigurational resonance states: “strong” $3d^9 5p$ (R2), “weak” $3d^9 5p$ (R3) and $3d^9 6p_{3/2}$ (R4). The intensity of the weak resonance R3 amounts to 1/80 of the strong resonance R2. Therefore, we discuss below the results for the resonances R1, R2, and partly for R4.

To compute the amplitude for the direct channel, we used the sudden approximation where only the monopole excitation of the $4p$ electron is taken into account [20]. This approximation is adequate here because the photoelectron energy $\varepsilon \approx 60$ eV is substantially larger than the energy of the additionally excited $4p$ electron $\varepsilon_{4p} = 14.1$ eV. Within the sudden approximation, the direct transition amplitude is nonvanishing for the KrII $4p^4(L_0 S_0)5p^2 P$ basis states only. Therefore, accounting for the direct transitions will influence the excitation dynamics of those KrII $4p^4 5p(E_1 J_1 = 1/2, 3/2)$ states which are described by a large contribution of the $4p^4(L_0 S_0)5p^2 P_{1/2,3/2}$ basis state.

Interference within the resonance pathways (r - r) [the sum over R in Eq. (2)] and between the resonance and the direct pathways (r - d) results in the dependence of all

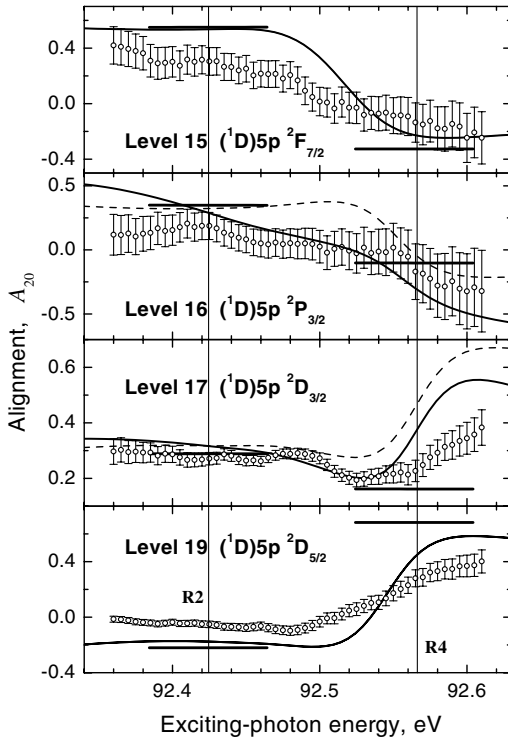


FIG. 1. Comparison of measured (open circles) and computed alignment for several KrII $4p^4 5p$ states. Solid and dashed lines: calculation with and without direct photoionization amplitude in Eq. (2). Horizontal bars with length equal to $\Gamma(R)$: A_{20} computed within the stepwise model. Vertical lines mark the positions of R2 and R4 resonances.

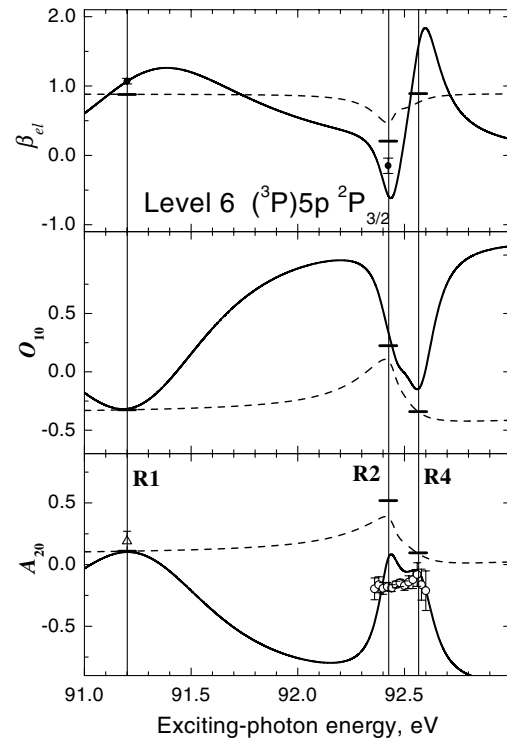


FIG. 2. Dependence of parameters β_{el} , A_{20} , and O_{10} on the exciting-photon energy. The line designation is as in Fig. 1. Dots with the error bars: measured β_{el} values [5]. Triangle: measured A_{20} value [9]. Open circles: present measurements. Vertical lines mark the positions of resonances.

the parameters β_{el} , A_{20} , and O_{10} on the exciting-photon energy ω . For some levels $|E_1 J_1\rangle$ the energy dependence of the A_{20} is shown in Fig. 1, while Fig. 2 displays the results for the set of β_{el} , A_{20} , and O_{10} (assuming positive helicity of exciting photons) parameters for the KrII $4p^4(L_0 S_0)5p^2 P_{3/2}$ level. The results computed by us within the stepwise model are presented in Figs. 1 and 2 as horizontal bars having a length equal to $\Gamma(R)$. Dashed and solid lines represent the results of calculations where the $(r-r)$ interference and $[(r-r) + (r-d)]$ interference are taken into account, respectively. Differences between the horizontal bars and the dashed lines at positions of resonances show the influence of the $(r-r)$ interference on the computed β_{el} , A_{20} , and O_{10} , whereas the differences between dashed and solid lines illustrate the influence of the $(r-d)$ interference in a pure form. Outside the widths of the resonances the $(r-d)$ interference is more important because the resonance amplitudes [the sum over R in Eq. (2)] become small for those energies.

As a first experimental test of the calculated dispersion, we measured the energy dependence of the alignment A_{20} for several states. The experiment was carried out at the undulator beam line UE56/2-PGM2 of BESSY II, Berlin, using photon-induced fluorescence spectroscopy [21,22]. The energy of the exciting synchrotron radiation was varied in steps of 5 meV covering the energy range from resonance $R2$ to $R4$ whose energies are 92.425 and 92.560 eV, respectively [17]. The bandwidth of the exciting radiation was 20 meV which, in view of the natural width of the KrI $3d^9 5p$ resonances of 83 meV [17,18], is in the Raman regime of excitation. The alignment has been determined by the setup and procedure described in

[9,15] and is based on the analysis of dispersed visible fluorescence radiation by using a Wollaston prism.

The A_{20} parameters determined in that way are plotted in Figs. 1 and 2. From the figures it is evident that the measured A_{20} values near resonances exhibit energy dependencies which were predicted by theory. In cases where the influence of the direct transition was expected to be large [states $(^3P)5p^2 P_{3/2}$ and $(^1D)5p^2 P_{3/2}$, see above], the experimental values definitely agree better with calculations incorporating the direct photoionization channel. Figures 1 and 2 show that the absolute values of the measured alignment are systematically lower than the computed ones. This is due to disalignment/disorientation effects. Among the Kr isotopes, the natural fraction of 11.5% of ^{83}Kr has only nonzero nuclear spin, namely, $I = 9/2$. Hyperfine interaction leads to disalignment factors for the isotopic mixture, computed as in [10], of 0.909, 0.911, and 0.913 for the ion J_1 values of 3/2, 5/2, and 7/2, respectively. Similarly, disorientation factors of 0.924, 0.926, 0.929, and 0.934 were calculated for $J_1 = 1/2, 3/2, 5/2,$ and $7/2$, respectively. The disalignment/disorientation factor due to radiative cascades was estimated using the transition array technique as in [15] and results in an average value of 0.913.

Table I summarizes the results of our calculations for β_{el} , A_{20} , and O_{10} which were performed “sitting on resonance” with a “zero bandwidth” of exciting radiation. We listed the results for those $4p^4 np$ levels only where there are either reliable literature data (well resolved lines) for β_{el} or there are data from the present measurement for A_{20} . The same table lists the measured β_{el} values

TABLE I. Angular distribution parameters β_{el} of outgoing $\varepsilon\ell$ electrons [see scheme (1)], alignment A_{20} , and orientation O_{10} (assuming positive helicity of exciting photons) parameters for some $4p^4 5p$ ionic states of the Kr atom.

| No. | Final $4p^4 5p$ Ionic state | Binding energy, eV | Resonance R1 ($3d_{5/2}^9 5p_{3/2}$) $\omega = 91.200$ eV | | | | | Resonance R2 ($3d_{3/2}^9 5p$) $\omega = 92.424$ eV | | | | |
|-----------------|--------------------------------|--------------------------|---|-----------|----------|----------|--------------|---|----------|----------|----------------|----------------|
| | | | β_{el} | | A_{20} | O_{10} | β_{el} | | A_{20} | O_{10} | | |
| | | | Expt [5] | Theor [4] | | | Expt [5] | Theor [4] | | | Present theory | Present theory |
| 1 | $(^3P)5p^4 P_{5/2}$ | 30.616 | -0.97 ± 0.03 | -0.994 | -0.997 | 0.777 | 0.323 | -0.98 ± 0.02 | -0.987 | -0.967 | 0.777 | 0.279 |
| 2 | $(^3P)5p^4 P_{3/2}$ | 30.675 | 0.68 ± 0.13 | 1.057 | 0.896 | -0.084 | -0.529 | 0.61 ± 0.02 | 0.536 | 0.754 | -0.218 | -0.518 |
| 5 | $(^3P)5p^2 P_{5/2}$ | 30.867 | -0.95 ± 0.02 | -0.991 | -0.992 | 0.798 | 0.309 | | 0.289 | -0.337 | 0.300 | -0.204 |
| 6 | $(^3P)5p^2 P_{3/2}$ | 31.121 | 1.07 ± 0.04 | 0.804 | 1.067 | 0.102 | -0.316 | -0.15 ± 0.11 | 0.962 | -0.584 | 0.054 | 0.343 |
| 7 | $(^3P)5p^2 P_{1/2}$ | 31.246 | 0.7 ± 0.2 | 0.395 | 0.848 | ... | -0.403 | -0.5 ± 0.2 | 0.704 | -0.069 | ... | -0.301 |
| 12 | $(^3P)5p^2 D_{3/2}$ | 31.576 | 1.04 ± 0.05 | 0.847 | 1.072 | -0.207 | -0.644 | -0.47 ± 0.02 | -0.675 | -0.131 | 0.032 | -0.280 |
| 13 | $(^3P)5p^2 S_{1/2}$ | 31.624 | 0.73 ± 0.07 | 0.270 | 0.933 | ... | -0.371 | | 0.676 | -0.777 | ... | 0.556 |
| 14 | $(^1D)5p^2 F_{5/2}$ | 32.565 | -0.8 ± 0.2 | -0.796 | -0.706 | 0.577 | 0.253 | -0.03 ± 0.14 | 0.344 | 0.020 | -0.116 | -0.431 |
| 15 | $(^1D)5p^2 F_{7/2}$ | 32.609 | 0.20 ± 0.06 | 0.280 | 0.208 | -0.292 | -0.693 | -0.98 ± 0.02 | -0.844 | -0.779 | 0.535 | 0.380 |
| 16 | $(^1D)5p^2 P_{3/2}$ | 32.677 | 0.64 ± 0.08 | 0.290 | 0.554 | -0.116 | -0.510 | 1.01 ± 0.10 | -0.365 | 0.674 | 0.290 | 0.346 |
| 17 ^a | $(^1D)5p^2 D_{3/2}$ | 32.880 | | -0.891 | -0.420 | 0.166 | -0.160 | | 0.742 | 0.708 | 0.316 | 0.023 |
| 18 | $(^1D)5p^2 P_{1/2}$ | 32.882 | 0.24 ± 0.07 | 1.204 | 1.535 | ... | -0.171 | 0.52 ± 0.13 | 0.688 | 1.304 | ... | -0.400 |
| 19 | $(^1D)5p^2 D_{5/2}$ | 32.889 | | -0.805 | -0.813 | 0.604 | 0.255 | | -0.573 | -0.672 | -0.176 | 0.667 |
| 20 | $(^1S)5p^2 P_{1/2}$ | 34.940 | | -0.253 | 0.600 | ... | -0.376 | 1.11 ± 0.09 | 1.006 | 1.033 | ... | -0.500 |
| 21 | $(^1S)5p^2 P_{3/2}$ | 35.010 | 0.86 ± 0.09 | 0.840 | 0.860 | -0.198 | -0.668 | | -0.802 | -0.150 | 0.614 | 0.267 |

^aLines (17–19) are not resolved in electron experiment [5].

as well as the results from [4] obtained within the stepwise model. In case of weakly resolved lines (17–19), the earlier experiment [5] gives one value. Therefore, we list in italics the value “weighted” over the levels (17–19). Table I demonstrates that accounting for the interference effects significantly improves the agreement between calculated and measured β_{el} [see, e.g., levels 7 (*R1* and *R2*), 14 (*R2*), 16 (*R1* and *R2*)]. In order to enable an overall comparison between the stepwise calculation [4] and the present one, we estimated the standard deviation between computed and measured [5] data for *all lines*. For the exciting-photon energy at both resonances *R1* and *R2*, the standard deviation for the computed data of [4] is equal to 0.237 and 0.692, respectively, whereas for the present calculation it is reduced to 0.115 and 0.290. If, however, the interference between resonance channels only is accounted for, the standard deviations calculated within the two-step model change by no more than 1.5%. Consequently, the dominant improvement of the agreement with experiment is due to the incorporation of the interference between the resonance and direct channels.

In conclusion, we calculated and observed for the first time the energy dependence of the alignment A_{20} for the $\text{KrII } 4p^45p$ states excited on the $\text{KrI } 3d^9np_j$ resonances in the Raman regime. Energy dependencies of the β_{el} and the O_{10} orientation parameters along the $\text{KrI } 3d^9np_j$ resonances were also predicted. The origin of the observed dispersion is the interference between different resonance channels and the direct photoionization channel. Therefore, it is stressed that the precise measurement of the energy dependence of β_{el} , A_{20} , and O_{10} within the Raman regime of excitation is essential to study electron correlation effects rather than measurements at one fixed energy, and some conclusions drawn from previous measurements in literature (e.g., [3–5,9,10]) should be reconsidered in view of the presently found energy dependence.

*Electronic address: vls@aanet.ru

†Electronic address: agschmor@rhrk.uni-kl.de

- [1] W. Eberhardt, G. Kalkoffen, and C. Kunz, *Phys. Rev. Lett.* **41**, 156 (1978).
- [2] G.B. Armen, H. Aksela, T. Åberg, and S. Aksela, *J. Phys. B* **33**, R49 (2000).
- [3] U. Hergenbahn, N.M. Kabachnik, and B. Lohmann, *J. Phys. B* **24**, 4759 (1991).
- [4] J. Tulkki, H. Aksela, and N.M. Kabachnik, *Phys. Rev. A* **50**, 2366 (1994).
- [5] H. Aksela, J. Jauhiainen, E. Nömmiste, S. Aksela, S. Sundin, A. Ausmees, and S. Svensson, *Phys. Rev. A* **54**, 605 (1996).
- [6] N.M. Kabachnik and I.P. Sazhina, *J. Phys. B* **9**, 1681 (1976).
- [7] A. Menzel, S.P. Frigo, S.B. Whitfield, C.D. Caldwell, M.O. Krause, J.Z. Tang, and I. Shimamura, *Phys. Rev. Lett.* **75**, 1479 (1995).
- [8] T.W. Gorczyca and F. Robicheaux, *Phys. Rev. A* **60**, 1216 (1999).
- [9] B. Zimmermann, O. Wilhelmi, K.-H. Schartner, F. Vollweiler, H. Liebel, A. Ehresmann, S. Lauer, H. Schmoranzer, B.M. Lagutin, I.D. Petrov, and V.L. Sukhorukov, *J. Phys. B* **33**, 2467 (2000).
- [10] M. Meyer, A. Marquette, A.N. Grum-Grzhimailo, U. Kleiman, and B. Lohmann, *Phys. Rev. A* **64**, 022703 (2001).
- [11] R. Camilloni, M. Žitnik, C. Comicioli, K.C. Prince, M. Zaccagna, C. Crotti, C. Ottaviani, C. Quaresima, P. Perfetti, and G. Stefani, *Phys. Rev. Lett.* **77**, 2646 (1996).
- [12] E. Kukk, H. Aksela, A. Kivimäki, J. Jauhiainen, E. Nömmiste, and S. Aksela, *Phys. Rev. A* **56**, 1481 (1997).
- [13] N. Saito, N.M. Kabachnik, Y. Shimizu, H. Yoshida, H. Ohashi, Y. Tamenori, I.H. Suzuki, and K. Ueda, *J. Phys. B* **33**, L729 (2000).
- [14] G.S. Brown, M.H. Chen, B. Crasemann, and G.E. Ice, *Phys. Rev. Lett.* **45**, 1937 (1980).
- [15] B.M. Lagutin, I.D. Petrov, Ph.V. Demekhin, V.L. Sukhorukov, F. Vollweiler, H. Liebel, A. Ehresmann, S. Lauer, H. Schmoranzer, O. Wilhelmi, B. Zimmermann, and K.-H. Schartner, *J. Phys. B* **33**, 1337 (2000).
- [16] V. Schmidt, *Rep. Prog. Phys.* **55**, 1483 (1992).
- [17] G.C. King, M. Tronc, F.H. Read, and R.C. Bradford, *J. Phys. B* **10**, 2479 (1977).
- [18] O.-P. Sairanen, A. Kivimäki, E. Nömmiste, H. Aksela, and S. Aksela, *Phys. Rev. A* **54**, 2834 (1996).
- [19] R. Kau, I.D. Petrov, V.L. Sukhorukov, and H. Hotop, *Z. Phys. D* **39**, 267 (1997).
- [20] V.L. Sukhorukov, A.N. Hoppersky, I.D. Petrov, V.A. Yavna, and V.F. Demekhin, *J. Phys. (Paris)* **48**, 1677 (1987).
- [21] A. Ehresmann, F. Vollweiler, H. Schmoranzer, V.L. Sukhorukov, B.M. Lagutin, I.D. Petrov, G. Mentzel, and K.-H. Schartner, *J. Phys. B* **27**, 1489 (1994).
- [22] H. Schmoranzer, H. Liebel, F. Vollweiler, R. Müller-Albrecht, A. Ehresmann, K.-H. Schartner, and B. Zimmermann, *Nucl. Instrum. Methods Phys. Res., Sect. A* **467–468**, 1526 (2001), and references therein.